Diagn Interv Radiol 2014; 20:209-221

ABDOMINAL IMAGING
REVIEW

MRI of hepatocellular carcinoma: an update of current practices

Hina Arif-Tiwari, Bobby Kalb, Surya Chundru, Puneet Sharma, James Costello, Rainner W. Guessner, Diego R. Martin

ABSTRACT
Hepatocellular carcinoma (HCC) is one of the most common cancers worldwide, and liver transplantation is the optimal treatment for selected patients with HCC and chronic liver disease (CLD). Accurate selection of patients for transplantation is essential to maximize patient outcomes and ensure optimized allocation of donor organs. Magnetic resonance imaging (MRI) is a powerful tool for the detection, characterization, and staging of HCC. In patients with CLD, the MRI findings of an arterial-enhancing mass with subsequent washout and enhancing capsule on delayed interstitial phase images are diagnostic for HCC. Major organizations with oversight for organ donor distribution, such as The Organ Procurement and Transplantation Network (OPTN), accept an imaging diagnosis of HCC, no longer requiring tissue biopsy. In patients that are awaiting transplantation, or are not candidates for liver transplantation, localized therapies such as transarterial chemoembolization and radiofrequency ablation may be offered. MRI can be used to monitor treatment response. The purpose of this review article is to describe the role of imaging methods in the diagnosis, staging, and follow-up of HCC, with particular emphasis on established and evolving MRI techniques employing nonspecific gadolinium chelates, hepatobiliary contrast agents, and diffusion weighted imaging. We also briefly review the recently developed Liver Imaging Reporting and Data System (LI-RADS) formulating a standardized terminology and reporting structure for evaluation of lesions detected in patients with CLD.

From the Departments of Medical Imaging (H.A.T., B.K., S.C., P.S., J.C., D.R.M. ✉ *dmartin@radiology.arizona.edu*), and Surgery (R.W.G.), University of Arizona College of Medicine, Tucson, Arizona, USA.

Received 12 September 2013; revision requested 11 October 2013; final revision received 21 November 2013; accepted 22 November 2013.

Published online 10 April 2014.
DOI 10.5152/dir.2014.13370

Hepatocellular carcinoma (HCC) is a major worldwide health concern; it is the sixth most common cancer and third leading cause of overall cancer-related mortality. HCC frequently presents as a rapidly growing tumor and has historically been associated with poor prognosis and outcomes. However, tumor screening protocols in high risk patients can lead to an earlier detection of treatable disease. Screening for HCC has resulted in significant improvements in the one-year cause-specific survival rates for new patients (1), and this is directly attributed to improved survival through the detection of early stage tumor.

The five-year cumulative risk of HCC ranges from 4%–30% in patients with chronic liver disease (CLD) and cirrhosis (2–3). Multiple therapeutic strategies are available for the treatment of HCC, including medical therapy, percutaneous tumor ablation, transarterial embolic therapy, surgical resection, and liver transplantation. Of all the available methods, liver transplantation is the most effective treatment for early HCC because this method removes not only the tumor but also the entire cirrhotic liver, which is at an increased risk for developing metachronous tumors. The effectiveness of liver transplantation depends upon detecting early stage disease within specific criteria. A seminal paper by Mazzaferro et al. (4), published in 1996, established the "Milan criteria" as the most widely used guidelines for transplant eligibility. The Milan transplant criteria has shown good outcomes in patients with a single tumor <5 cm, or up to three tumors but with none greater than 3 cm, without extrahepatic spread or signs of vascular invasion. These criteria yield overall and recurrence-free survival rates of 85% and 92%, respectively, at four years after orthotopic liver transplantation (4). These survival rates are similar to patients transplanted for nonmalignant indications at four years following surgery; thus, accurate staging is mandatory for proper inclusion in the transplant list.

Numerous studies have been performed to investigate the diagnostic accuracy of ultrasonography (US), computed tomography (CT), or magnetic resonance imaging (MRI). In this review, we discuss MRI acquisition methodology, reporting methods and provide a discussion of the varied appearance of HCC.

Imaging methods for screening

Ultrasonography

US is used for HCC surveillance in CLD at many centers, primarily due to ease of access, lack of ionizing radiation, and relative lower initial per study cost compared with CT and MRI. However, reports indicate highly variable sensitivity for the detection of HCC with US, ranging from 33% to 96% (5). Multiple studies have shown a lower detection rate of HCC by

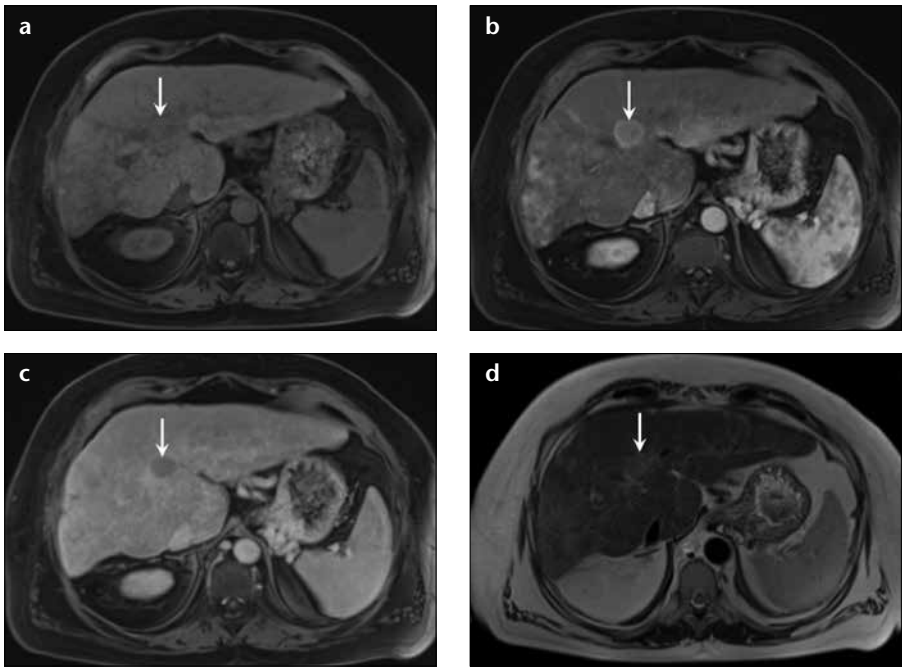

Figure 1. a–d. A 50-year-old man with hepatitis C infection and HCC, and prior negative screening US. Axial precontrast **(a)**, arterial **(b)**, and delayed phase **(c)** T1-weighted 3D GRE images, and T2-weighted single-shot image without fat suppression **(d)** demonstrate an isointense lesion in segment VIII on precontrast T1-weighted 3D GRE (**a,** *arrow)*, which shows avid enhancement on the arterial phase (**b,** *arrow*) and washout on the delayed phase (**c,** *arrow*) with an enhancing capsule. Mildly increased signal is observed on T2-weighted nonfat-saturated single-shot images (**d,** *arrow*); all these features are characteristic of HCC. The tumor burden was within the Milan criteria, and the patient underwent a successful transplantation.

US when compared with CT or MRI (Fig. 1) (6). In addition, the sensitivity for the detection of dysplastic nodules and small HCC is poor; regenerative nodules, dysplastic nodules, and small HCC may be indistinguishable by US (7). The use of contrast-enhanced US with microbubbles improves the diagnostic performance of US; however, the use of US contrast adds both time and cost to the test, and is not yet approved for use in all countries, including the USA.

The cost-effectiveness of US for HCC surveillance has been questioned. For example, Kim et al. (8) evaluated 100 patients that developed HCC while receiving surveillance US and who had prior negative US examinations with the appropriate time interval between scans; up to 30% of these patients presented with tumor stage outside of surgical treatment options such as transplantation or surgical resection.

Computed tomography

The use of multidetector CT for the detection of HCC requires an optimized triple-phase technique that includes image acquisition during multiple phases of contrast enhancement to evaluate for the distinctive findings of arterial enhancement and delayed washout characteristics of HCC (9). Some studies have suggested a lower sensitivity for dysplastic nodules, small HCC, and infiltrative-HCC compared with MRI (Fig. 2) (5). Large, prospective multicenter trials comparing the accuracy of CT and MRI for HCC detection are not yet available; however, the American College of Radiology Imaging Network is currently conducting a prospective multicenter trial (ACRIN 6690) designed to address this issue. The repeated use of CT for screening raises concerns with regard to cumulative X-ray dose effects. In addition, a subset of patients with hepatorenal disease may be at increased risk for worsening renal function from iodinated contrast exposure (10).

Magnetic resonance imaging

Multiple studies have demonstrated excellent sensitivity and specificity of MRI for the detection and characterization of HCC (11–14), particularly for smaller tumors, 1–2 cm in size with sensitivity up to 84% and 47% with MRI and CT, respectively (Fig. 3) (7, 13). Our own recent analysis of liver explant pathology versus prospective MRI staging of HCC demonstrated 97% sensitivity and 100% specificity for the detection of HCC. The detection rate of smaller (<2 cm) tumors, in particular, was noted to have improved from 55.6% in 2006 to 87.5% in 2010, largely secondary to technology updates related to graded improvements in MR sequence design and hardware (15). It should also be emphasized that this study was performed using prospective clinical interpretations from individual radiologists, unlike most studies that have used retrospective readings by one or more radiologists; prospective interpretations provides a better estimate of true performance of a test in a natural clinical environment. MRI has several advantages over CT that includes greater safety, no ionizing radiation, no risk of kidney damage, no known cases of nephrogenic systemic fibrosis in patients scanned with CLD (16), probable better sensitivity and specificity particularly for smaller tumors and diffuse HCC, more consistent and better visualization of tumor involvement of the portal vein with better differentiation of tumor from bland thrombus (5, 17).

MRI and HCC: technical considerations

MRI protocols for HCC surveillance should be standardized and uniform, with strategies that allow clinicians and technologists to perform repeatable, high quality examinations that retain diagnostic quality even in patients with difficulty in breath-holding. Optimized technique is anchored on dynamic, fat-suppressed gadolinium-based contrast agent (GBCA) enhanced T1-weighted three-dimensional gradient-echo (3D GRE) sequences, combined with motion insensitive, single shot T2-weighted images with and without fat suppression.

MRI protocol

Core techniques

Detection of focal HCC relies most heavily on dynamic, multiphase T1-weighted 3D GRE sequences, and

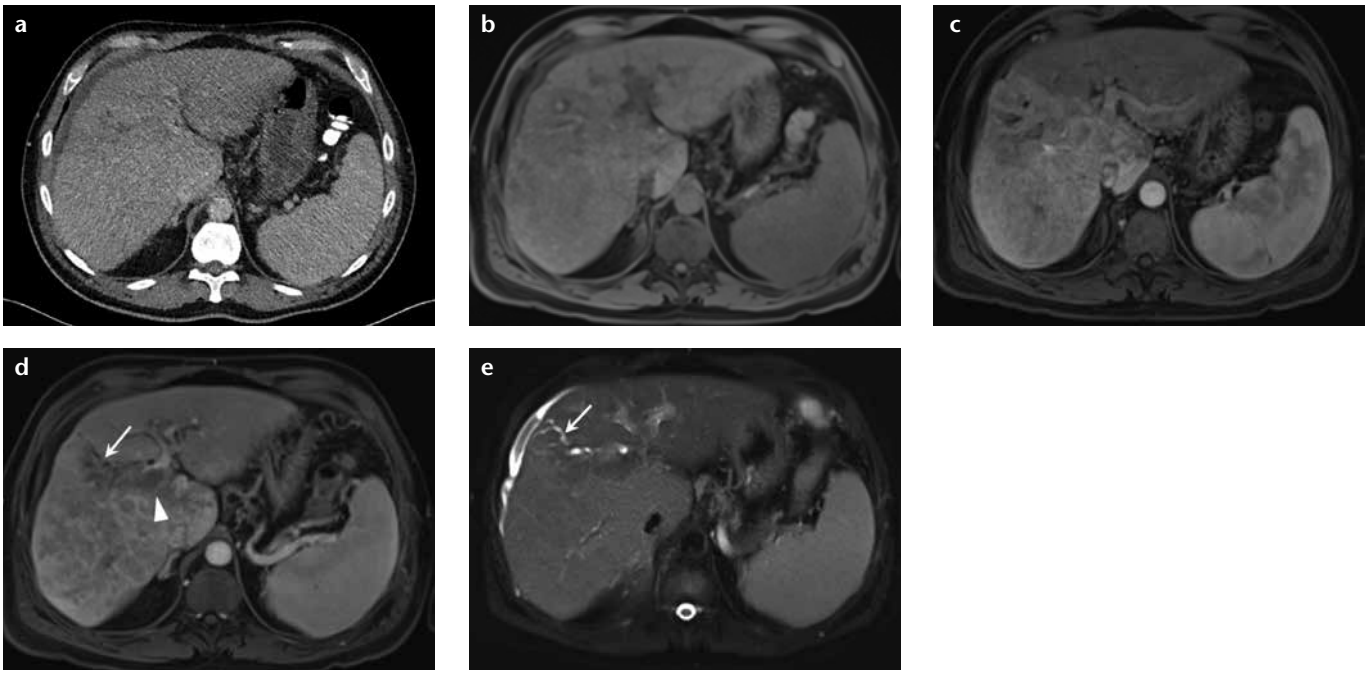

Figure 2. a–e. A 50-year-old man with abdominal pain. Axial single phase CT from another institution **(a)** shows slight irregularity of the hepatic surface, mild biliary dilatation, and trace ascites. MRI of abdomen was subsequently performed to identify the cause of biliary obstruction. Unenhanced T1-weighted 3D GRE image **(b)** demonstrates heterogeneous signal pattern to the hepatic parenchyma. Gadolinium-enhanced arterial phase image **(c)** shows diffuse, nonuniform enhancement throughout the right hepatic lobe, but without a focal lesion. Delayed-phase postcontrast image **(d)** shows heterogeneous, nonuniform pattern of enhancement and areas of washout. Single-shot, fat-suppressed axial T2-weighted image **(e)** reveals abnormal, geographic regions of elevated T2 signal representing diffuse infiltrating HCC. Tumor thrombus is observed to extend into the main portal vein (**d,** *arrowhead*). Infiltrative tumor obstructs the biliary duct in the right lobe of the liver causing segmental biliary ductal obstruction (**d, e,** *arrows).*

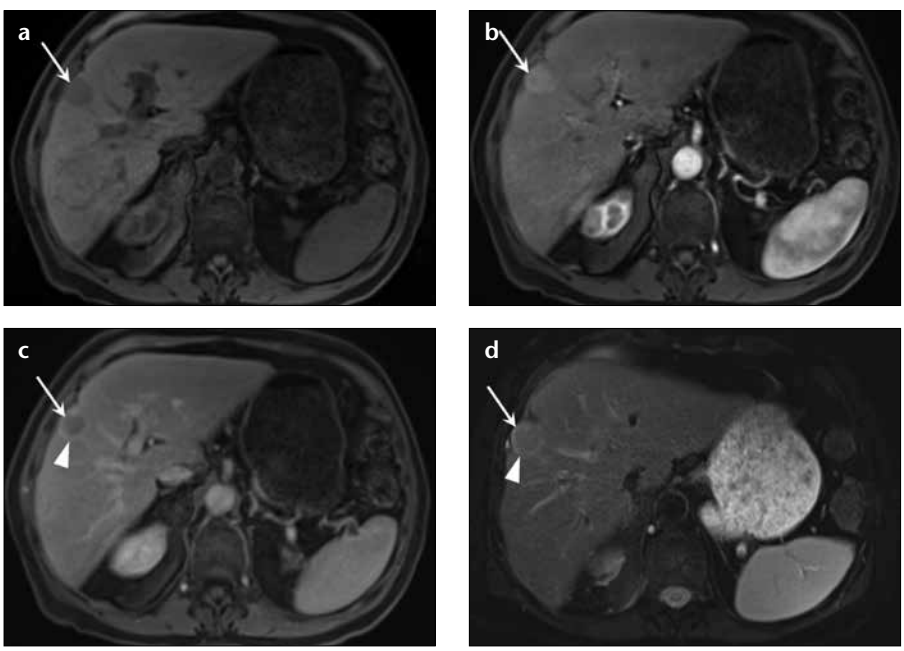

Figure 3. a–d. A 85-year-old man with hepatitis C infection presents with liver mass. Precontrast **(a)** and arterial phase **(b)** 3D GRE images show arterial enhancement of the tumor in the right lobe of the liver (**a, b,** *arrows*). Delayed phase 3D GRE image **(c)** depicts washout *(arrow)* and capsule enhancement *(arrowhead)*. T2-weighted fat-saturated single-shot image **(d)** shows mildly elevated T2 signal intensity within the tumor *(arrow)* and tumor capsule *(arrowhead)*.

proper timing of the arterial phase is crucial for optimizing sensitivity for HCC detection (Fig. 4). GBCA perfusion of arterial-vascularized tumors is a transient phenomenon, and errors of only a few seconds during the arterial phase image acquisition may render an exam less diagnostic for HCC detection. While multiple arterial timing strategies have been investigated (18), real-time, bolus-tracking methods that provide arterial phase images tailored to an individual patient's cardiac output and blood volume have numerous advantages, including reducing overall scanning time. A real time bolus-triggered method has been described with breath-hold instructions initiated as the contrast bolus reaches the celiac trunk (trigger point), and imaging initiated at an 8–10 s delay from the trigger point (19). Acquisition time for 3D GRE imaging through the liver and abdomen is typically within 15–18 s, obtained during a single breath-hold. While exact timing of the additional phases of contrast is less important, venous phase imaging may then be initiated at 40–70 s and delayed phase imaging at 120–300 s after the trigger point to obtain the additional necessary diagnostic information.

The Organ Procurement and Transplantation Network (OPTN) committee has recommended minimum technical specifications for dynamic contrast-enhanced MRI of the liver, which are outlined in Table 1 (20).

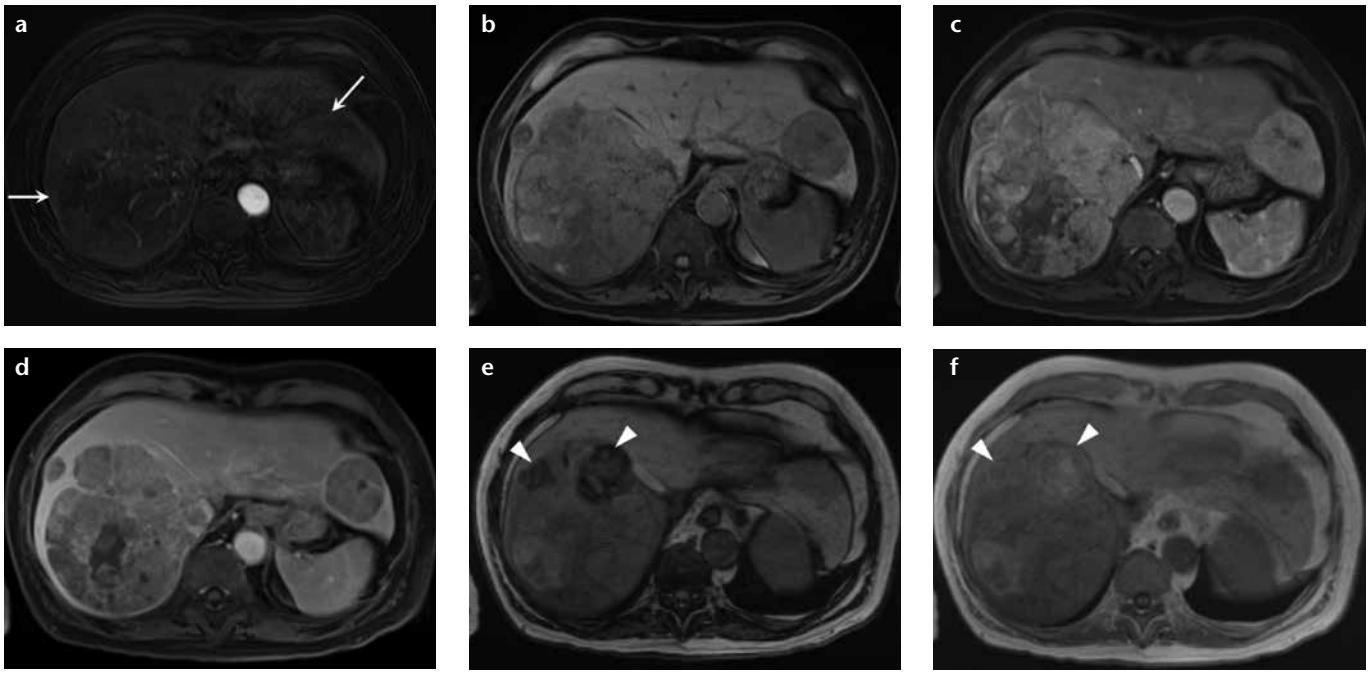

Figure 4. a–f. An 85-year-old man with multifocal HCC. An outside examination with a poorly timed arterial phase **(a)** fails to show the typical vascularity of HCC due to an early phase of contrast; follow-up MRI was then performed with proper timing. Precontrast **(b)**, arterial **(c)**, and delayed phase **(d)** T1-weighted 3D GRE images show arterial enhancement in multiple tumors in both lobes of the liver with subsequent washout. Dual echo T1-weighted GRE images show loss of signal on the out-of-phase image (**e,** *arrowheads)* compared with the in-phase images (**f,** *arrowheads),* consistent with internal lipid within the tumor, a feature characteristic of HCC.

Protocol

We have previously described our techniques (15, 19). We recorded each patient's weight and administered gadobenate dimeglumine (MultiHance, Bracco Diagnostics, Princeton, New Jersey, USA) at a dose of 0.05 mmol/kg and an injection rate of 2 mL/s, followed by a 30-mL saline flush (also at 2 mL/s) using a dual-chamber power injector, with the objective of minimizing gadolinium dose while preserving R1 effects of a standard agent dose (16). We used a real time bolus-triggered technique to acquire the arterial phase (19), followed by venous (60 s) and delayed phase (180 s) images. This contrast dosing strategy has been shown to retain excellent accuracy with respect to HCC detection (15).

T2-weighted images may be acquired with a single-shot fast spin-echo technique in the coronal and axial plane without fat saturation, and in the axial plane with fat saturation using a spectral adiabatic inversion recovery (SPAIR) technique (21, 22). While T2-weighted sequences are not critical for the diagnosis of the majority of focal HCC, the more aggressive infiltrative subtype of HCC is frequently best demonstrated on T2-weighted images. A breath-hold (end inspiration) dual-echo spoiled GRE sequence is also performed for qualitative evaluation of tissue fat and iron and to best define features that may be important when evaluating a subset of focal liver lesions in the setting of CLD.

New and developing techniques

Hepatobiliary specific agents

Recently, a new gadolinium based chelate agent, gadoxetate disodium (Gd-EOB-DTPA, Eovist/Primovist, Bayer Pharmaceuticals,), has been introduced with altered uptake and excretion pathways relative to standard agents. Gd-EOB-DTPA demonstrates 50% uptake (through an active transport mechanism) and excretion by the normal liver into the bile ducts. This manifests as an increased signal in the hepatic parenchyma on T1-weighted images that peaks at approximately 20 min postinjection. G-EOB-DTPA has been advocated for use in the diagnosis of HCC, with the concept that carcinoma cells will not express the anion-transporting peptide to accumulate the gadolinium agent; tumor should then present as a focus of hypointense signal against the remainder of the hepatic parenchyma that expresses this transporter and takes up the Gd-EOB-DTPA. However, the routine use of this agent for HCC screening remains controversial, with contradicting results published in the literature. Approximately 10%–15% of HCC may retain contrast on delayed hepatobiliary phase images, thereby appearing isointense or hyperintense to background hepatic parenchyma, enhancement features that are similar to benign regenerative or dysplastic nodules (7, 23). In addition, liver uptake will be impaired in patients with active or more advanced CLD yielding potentially variable hepatic phase enhancement (23). The cost of Gd-EOB-DTPA can be significantly higher than other GBCAs, which is an important consideration with regards to cost-effectiveness considerations. Overall, continued investigations with more direct comparative analysis between Gd-EOB-DTPA and other extracellular agents are warranted.

Diffusion-weighted imaging

Additional MR methods have been proposed to improve the detection of HCC, including diffusion-weighted imaging (DWI). Some authors have shown encouraging results for improved sensitivity of HCC detection,

Table 1. The Organ Procurement and Transplantation Network (OPTN) recommendations for minimum technical specifications for dynamic contrast-enhanced MRI of the liver.

Feature	Specification	Comment
Scanner type	1.5 Tesla or greater main magnetic field strength	Low field magnets are not suitable
Coil type	Phased array multichannel torso coil	Unless patient-related factors precludes use (e.g. body habitus)
Minimum sequences	Precontrast and dynamic post gadolinium T1-weighted gradient echo sequence (3D preferable) T2-weighted (with and without fat saturation) T1-weighted in- and out-of-phase imaging	
Injector	Dual chamber power injector	Bolus tracking is recommended
Contrast injection rate	2-3 mL/s of extracellular gadolinium chelate that does not have dominant biliary excretion	Preferably resulting in vendor-recommended total dose
Mandatory dynamic phases on contrast enhanced MRI (comments describe typical hallmark image features)	a) Precontrast T1-weighted b) Late arterial phase c) Portal venous phase d) Delayed phase	a) Do not change scan parameters for postcontrast imaging b) Artery fully enhanced, beginning contrast enhancement of portal vein c) Portal vein enhanced, peak liver parenchymal enhancement, beginning contrast enhancement of hepatic veins d) Variable appearance, >120 s after initial injection of contrast
Dynamic phases (timing)	The use of a bolus tracking method for timing contrast arrival for late arterial phase imaging is preferable. Portal venous phase (35–55 s after initiation of late arterial phase scan), delayed phase (120–180 s after initial contrast injection)	
Slice thickness	5 mm or less for dynamic series, 8 mm or less for other imaging	
Breath-holding	Maximum length of series requiring breathhold should be about 20 s with a minimum matrix of 128×256	Compliance with breathhold instructions is very important, technologists need to understand the importance of patient instruction before and during scan

3D, three-dimensional; MRI, magnetic resonance imaging.

mostly for some well-differentiated HCC with atypical postcontrast imaging features (24). Complementary to conventional MRI, a lesion on DWI is suspicious for HCC when it shows sustained, elevated signal relative to the surrounding liver parenchyma with increasing b factors (b=50, 400, and 800 s/mm^2) and a nearly equivalent or lower apparent diffusion coefficient compared with the background parenchyma on the ADC map (24, 25).

Additional diagnostic information in characterizing and differentiating HCC can be extracted from rapid perfusion imaging with multiple arterial phases (26, 27). Newer methods for accelerated acquisition of 3D GRE are being proposed that use techniques, such as highly under-sampled radial methods, which can be further combined with shared k-space methods (28, 29).

The new sequences and contrast agents remain under continued development and investigation. Any developing method that is proposed to improve HCC detection rate should be compared against the reference standard of optimized, dynamic T1-weighted GRE with individually tailored arterial phase timing, which has shown sensitivities and specificities of >90%–95% in the peer-reviewed literature (15, 30–32).

MRI and HCC: imaging features

Cirrhotic nodules undergo carcinogenesis along a spectrum, ranging from benign regenerative nodules to dysplastic nodules to malignant HCC. The change in vascularity of the nodules during this process correlates with the development of malignancy, and determines their distinguishing imaging characteristics (Table 2).

Regenerative nodules

Regenerative nodules are composed of proliferating normal hepatic parenchyma surrounded by intervening fibrous stroma. Regenerative nodules primarily draw their blood supply from the portal vein, and therefore appear similar to background hepatic parenchyma on all MR sequences, demonstrating isointense signal on T1- and T2-weighted images compared with the background hepatic parenchyma. Elevated T1 signal may be observed in regenerative nodules; the etiology for this finding remains uncertain, though postulated theories suggest the presence of lipid, protein, or possibly metal and/or metal-binding proteins. When iron is present in regenerative nodules, susceptibility effects can result in decreased signal intensity on both T1- and T2-weighted images. Regardless of their intrinsic signal features, a reliable finding of regenerative nodules is the absence of enhancement in the arterial phase, compared with the background hepatic parenchyma (3).

Dysplastic nodules

Regenerative nodules may undergo low to high grade dysplastic change, forming dysplastic nodules, which are found in 15%–25% of cirrhotic livers. While dysplastic nodules typically show T2 signal that is similar to the background liver, there may be variable signal on T1-weighted images, similar to regenerative nodules. The charac-

Table 2. MRI differentiation of nodules in chronic liver disease

Sequence	Regenerative	Dysplastic	HCC
T1-weighted 3D GRE			
Precontrast	↑ or iso	↑ or iso	↑, iso or ↓
Arterial enhancement	-	+	+
Delayed washout	-	-	+
T2-weighted (single shot)	iso	iso	↑ or iso
T1-weighted dual echo GRE, lipid			
(Loss of signal, out-of-phase)	-	-	+
DWI	-	-	- or +
Gadoxetate disodium	iso	iso	↓(majority) or ↑ (small percentage)

↑, increased signal relative to background hepatic parenchyma; ↓, decreased signal relative to background hepatic parenchyma; Iso, isointense signal relative to background hepatic parenchyma; +, present; -, absent; DWI, diffusion-weighted imaging; GRE, gradient echo; 3D, three-dimensional.

teristic feature of dysplasia is increased enhancement on arterial phase images relative to the background hepatic parenchyma. It is presumed that dysplastic nodules induce neo-angiogenesis of vessels derived from arterial supply and become increasingly enhanced in the arterial phase images relative to the degree of dysplasia. There is no washout on delayed phase imaging, using conventional extracellular GBCAs because supply from the portal venous system remains comparable with the adjacent liver (Fig. 5). Another characteristic of dysplasia is size of the lesion with most of these nodules smaller than 1–2 cm in maximum diameter (3). The presence of a small, less than 1–2 cm nodule that demonstrates increased enhancement in the arterial phase, without delayed phase washout or elevated T2 signal, may be considered to be a probable dysplastic nodule, and warrants more frequent surveillance imaging as there is an increased risk of progression to HCC. An increased three- to six-month's interval imaging frequency has been suggested (20).

Hepatocellular carcinoma

In CLD, HCC may appear as a solitary focal mass (50%), multifocal mass (40%), or diffusely infiltrative tumor (10%). Focal HCC demonstrates variable signal on T1-weighted imaging, ranging from hyperintense to hypointense. Intratumoral lipid is a relatively common characteristic observed with HCC histologically, and may be identified in a subset of cases on dual echo, T1-weighted GRE images, with loss of signal on the opposed-phase images compared with the in-phase images. The presence of lipid can be diagnostically helpful in lesions that have an otherwise atypical imaging appearance; any enhancing lesion with internal lipid in the setting of CLD may be presumed to represent HCC (Fig. 4).

Focal or multifocal HCC shows irregular, increased enhancement in the arterial phase, reflecting tumor neoangiogenesis that derives its blood supply nearly exclusively from the hepatic artery. On portal venous phase, HCC may be inconspicuous or begin to washout (i.e., becoming darker than the adjacent hepatic parenchyma). The key distinguishing feature between dysplastic nodules and HCC is the development of washout and a thick, enhancing capsule on delayed interstitial phase postcontrast images, secondary to the lack of portal supply to malignant nodules. Characteristically, the tumor capsule may be observed in approximately 80% of HCCs and corresponds on histology to a pseudocapsule consisting of compressed adjacent liver parenchyma with occasional nonspecific inflammatory cells (33).

Vascular invasion by HCC is a common feature that is observed microscopically and is identified on a subset of cases on MRI. The vascular invasion by tumor excludes liver transplantation; chemotherapy or chemoembolization represents treatment options. Macrovascular invasion most commonly involves the portal system and less commonly the hepatic veins. The pattern of HCC growth is highly characteristic. HCC invades and grows within the lumen, often distending the vein. This is distinctive from cholangiocarcinoma, a tumor that invades along the outer margins of the veins and occludes the vessels by constriction. On precontrast T2-weighted images, the normal dark blood appearance of the involved vein becomes higher in signal intensity. Balanced Fast Field Echo (BFFE), also called True-Free Induction fast Precession (T-FISP), images normally produce high signal from within the veins, becoming lower in signal when a tumor thrombus is present. Although useful, benign venous thrombus has the same appearance on precontrast images. Dynamic postcontrast imaging with a standard extracellular GBCA will show arterial enhancement within tumor thrombus and intermediate level signal on venous phase. Benign thrombus will remain relatively low in signal on arterial phase and become conspicuously lower in signal than the surrounding enhancing blood on venous phase, where the GBCA will outline conspicuously the margins of the benign thrombus. Gd-EOB-DTPA produces a different pattern of enhancement in that the liver adjacent to the portal or hepatic vein will become relatively enhanced, even at 1–3 min after administration, when compared with a standard GBCA. A malignant venous thrombus may be relatively less conspicuous on Gd-EOB-DTPA because the adjacent liver may enhance to a greater degree than the tumor thrombus effectively diminishing the tumor thrombus conspicuity.

The appearance of HCC on T2-weighted images is variable. Most commonly, HCC appears isointense to background liver on T2-weighted images. The elevated T2 signal in a focal lesion can be useful to reliably differentiate HCC from dysplastic nodules. When a focus of HCC develops within a dysplastic nodule, a mildly elevated signal may be observed on T2-weighted images, representing the focus of HCC within the low density dysplastic nodule, and has been described as a "nodule in nodule" appearance. Preliminary data from our institution suggests that the degree of T2 signal

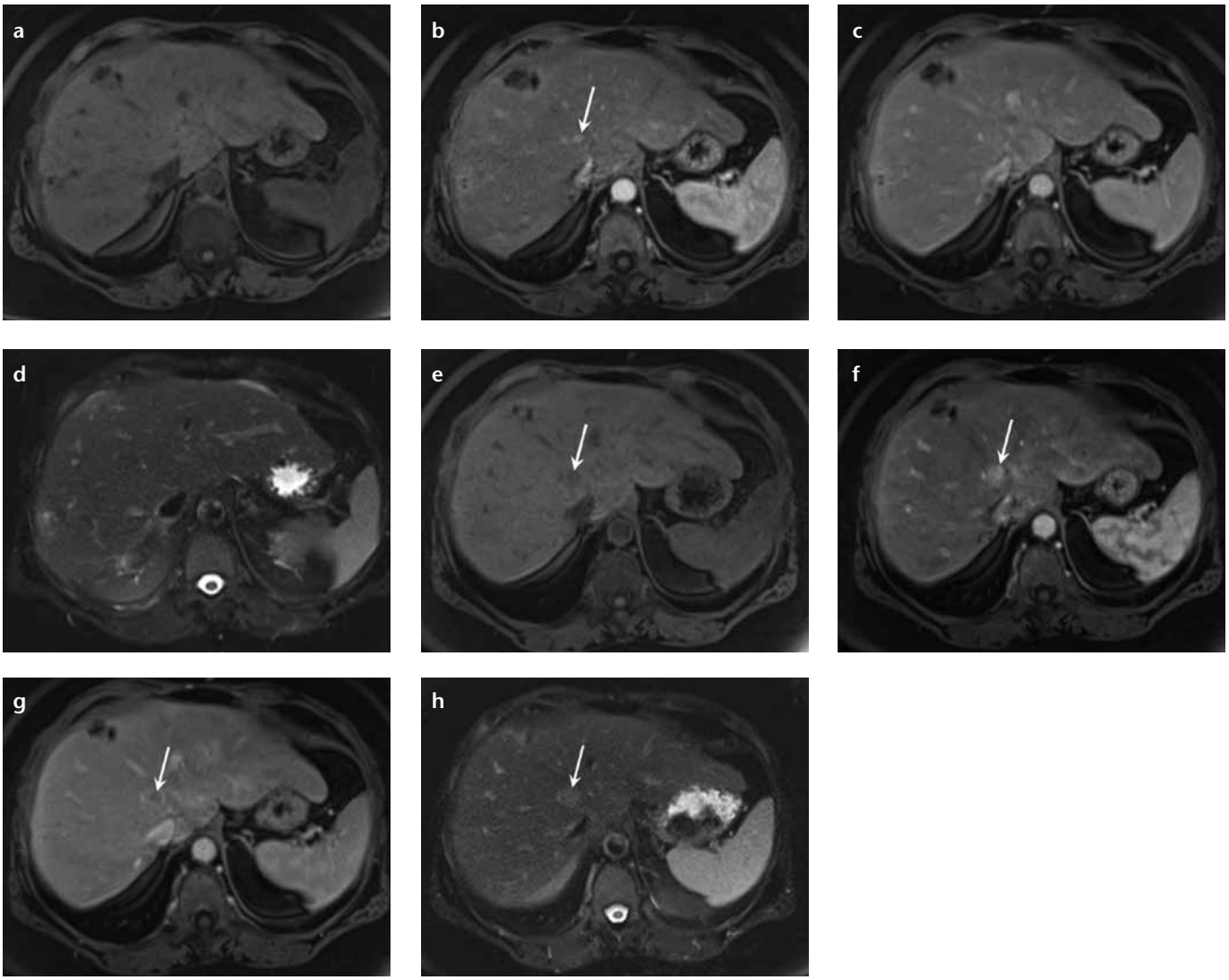

Figure 5. a–h. A 62-year-old woman with chronic liver disease, undergoing surveillance imaging for HCC. Precontrast **(a)** and arterial phase **(b)** T1-weighted 3D GRE images, show a small hyperenhancing nodule in the right lobe of the liver (**b,** *arrow*), with absence of washout on delayed phase **(c)** and no abnormal signal on T2-weighted fat-saturated single-shot images **(d)**; these features are in keeping with a dysplastic nodule. Note incidental postsurgical changes in anterior segment VIII. The follow-up MRI in three months interval on precontrast **(e)** and arterial phase **(f)** T1-weighted 3D GRE images reveal interval increase in size of the arterially enhancing hepatic nodule (**f, e,** *arrows*), which now demonstrates washout on delayed phase T1-weighted 3D GRE images (**g,** *arrow*). In addition, the lesion also now shows mildly elevated signal on T2-weighted fat-saturated single-shot images (**h,** *arrow*). Together with the above findings and data that state the consistent evolution of a dysplastic nodule into HCC, demonstrate the utility of MRI in depicting and following high risk, premalignant lesions in the setting of background chronic liver disease.

abnormality in HCC may correlate with the biologic behavior and risk of post-transplant tumor recurrence (34). DWI also may have some role in the prognostication of tumor recurrence, particularly for smaller lesions (35).

MRI features of infiltrative HCC (I-HCC) was first described by Kanematsu et al. in 2003 (36). I-HCC may be undetectable by other imaging modalities, particularly on US (37). In distinction to the solitary focal and multifocal subtypes, I-HCC may be nearly inconspicuous on postcontrast imaging, making I-HCC potentially a challenging diagnosis. Most I-HCCs are highly conspicuous on T2-weighted images showing high signal relative to the adjacent liver. In addition, MRI can readily show venous invasion, which is common to most I-HCCs.

Liver Imaging-Reporting and Data System and the Organ Procurement and Transplantation Network Committee

Imaging plays a critical role in identifying at risk patients to determine eligibility and priority for hepatic transplantation. The OPTN, through the United Network for Organ Sharing (UNOS), propose specific HCC imaging criteria for appropriate organ allocation (20). American Association for the Study of Liver Diseases (AASLD) published practice guidelines for the management of HCC. Identification of 1 cm or larger lesions in patients with CLD on screening or surveillance US should be followed by further imaging on either a multiphase CT or MRI to confirm the diagnosis of HCC.

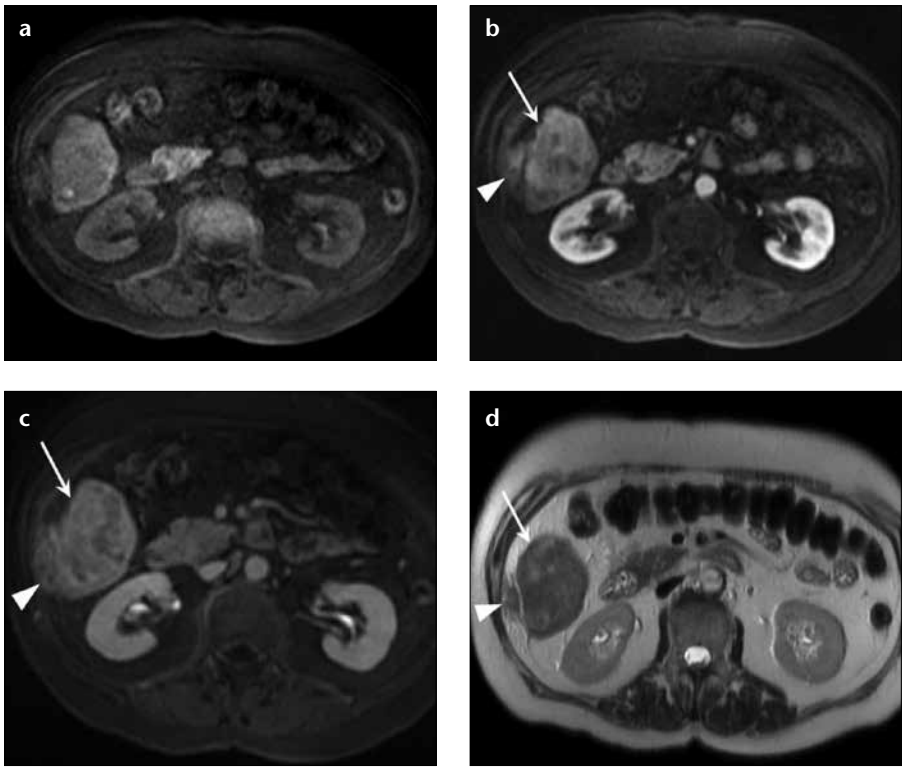

Figure 6. a–d. A 60-year-old male patient with HCC. A biopsy was performed at an outside institute to characterize a hepatic mass. The follow-up MRI in precontrast **(a)**, arterial **(b)**, delayed phase **(c)** T1-weighted 3D GRE images, and T2-weighted single-shot image **(d)** show a typical HCC in segment VI *(arrows)*. Enhancing tumor soft tissue, similar in signal pattern to HCC, is observed along the biopsy track extending from the liver capsule to the abdominal wall musculature, representing postbiopsy seeding *(arrowheads)*.

The Liver Imaging-Reporting and Data System (LI-RADS) is a new method of reporting endorsed by the American College of Radiology to formulate a standardized terminology and reporting structure for evaluation of lesions identified in patients with CLD. This nomenclature addresses the full spectrum of lesions and pseudolesions encountered on imaging of at risk patients; criteria for diagnosis of hypovascular and hypervascular HCC are outlined. Imaging details of various benign and malignant hepatic tumors are illustrated and non-HCC malignancies, like cholangiocarcinoma are also discussed. Hepatic lesions are categorized from LR1 to LR5 depending on imaging features to suggest whether the findings are definitely benign (LR1) or definitely malignant, i.e., HCC (LR5). The findings suggestive of, but not diagnostic of either a benign lesion or HCC are categorized as LR2 and LR4, respectively. LR3 is designated for lesions which have nonspecific and indeterminate features. Details of LI-RADS are outlined in Table 3 (38, 39). The overall approach and categorizations of tumor features in OPTN-UNOS are similar to those used for the LI-RADS system. The OPTN system uses a five-level classification and a tumor with features of HCC is designated as an OPTN class 5 lesion.

The role of liver biopsy

The excellent long-term results of transplantation for the treatment of HCC are highly dependent on accurate pretransplant staging of the disease because patients that underwent transplantation from outside the established criteria have shown significantly worse outcomes (4, 40). As discussed earlier, MRI provides highly accurate staging for HCC and there is rarely a need for percutaneous tumor biopsy using current transplant guidelines. Needle sampling of cirrhotic livers is an invasive technique with risks of bleeding and even death in rare cases. In addition, it is increasingly recognized that the risk of tumor seeding may represent a significant concern, particularly when there is postbiopsy bleeding (Fig. 6). The actual estimate of seeding frequency of HCC by biopsy is difficult to accurately assess; however, retrospective studies show 0%–5.1% frequency (median 2.7%) (41); when this occurs, a patient is converted from a transplant candidate to an incurable disease candidate. It may also be possible that a patient undergoes transplantation and peritoneal seeding becomes evident only after the procedure. Sampling error in biopsy (Fig. 7), particularly for smaller nodules in difficult locations (such as the hepatic dome), is well known, with an overall 10% false negative rate of diagnosis on biopsy. The failure of image guided percutaneous biopsy is observed in 3%–16% of cases, which may arise with inadequate sampling, and raises risks of false negative diagnosis, particularly in well differentiated HCC. The chances of success with repeat biopsy is relatively low when the deficiency is limited by characteristics of the lesions, such as areas of necrosis in large nodules or well differentiated cellular areas in small sized HCC, and increases the risk of bleeding and tumor seeding (42).

Major transplant organizations, including the UNOS and the European Society for Organ Transplantation (ESOT) no longer require histological confirmation of HCC prior to liver transplantation if a tumor shows characteristic features of HCC on imaging, either CT or MRI. Smaller lesions that are identified on imaging that do not meet full criteria for the diagnosis of HCC may be reimaged in 3–4 months, combined with a planned delay for liver transplantation if these additional tumors will stage an individual patient outside of the Milan criteria. Through this period, the nodule may develop the specific imaging features of HCC, which will obviate the need for a biopsy and provide the confirmatory diagnosis needed for pretransplant staging. Using longitudinal short-interval time-course imaging for staging in a patient with an indeterminate nodule is therefore now believed to be more accurate and safer than biopsies (41, 43).

MRI of percutaneous ablative methods and chemoembolization

Percutaneous therapy for HCC may be considered for selected patients as

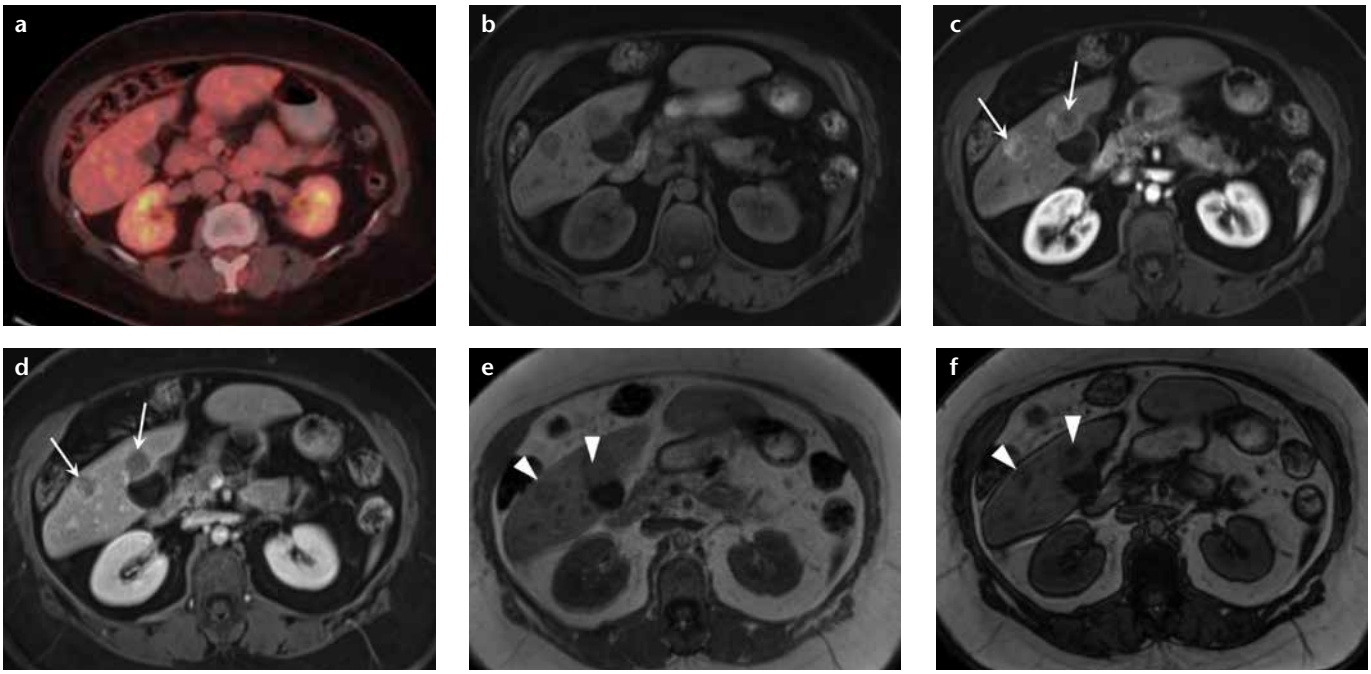

Figure 7. a–f. A 61-year-old woman with hepatic lesions, cancer workup. Multiple biopsies returned a diagnosis of neuroendocrine metastases. PET-CT **(a)** showed no increased fluorodeoxyglucose avidity in the hepatic lesions. Precontrast **(b)** and arterial phase **(c)** T1-weighted 3D GRE images show two arterially enhancing masses in the right lobe of the liver, which show prompt washout on delayed phase **(d)**. Dual echo T1-weighted GRE images **(e, f)** show focal areas of signal loss on the out-of-phase images (**e,** *arrowheads*) compared with the in-phase images (**f,** *arrowheads*), depicting internal lipid within the tumor. These findings are most consistent with HCC, despite the biopsy results. Special stains for HCC confirmed the diagnosis in the surgical specimen. This case demonstrates the value of MRI when used as a primary diagnostic modality for liver lesions, and HCC in particular. MRI may obviate the need for additional imaging tests and biopsy, potentially reducing overall cost while retaining high diagnostic accuracy.

a bridge to hepatic transplantation, when hepatic transplantation cannot be offered due to hepatic tumor burden outside of the Milan criteria, and also when tumor resection is a risk in patients with poor hepatic reserve. The percutaneous treatment methods may be divided into arterial delivery of a tumor cytotoxic agent (transarterial chemoembolization and/or yttrium-90 [Y-90] microspheres) versus direct tissue infarction through the use of microwave energy, radiofrequency heating, or cryoablation. Pretreatment imaging is crucial for procedural planning specifically to identify the extent of tumor and to assess the distribution of adjacent structures relative to the tumor, such as the hepatic or portal veins (which may decrease treatment efficacy by acting as a heat sink) and bile ducts or bowel (to avoid unwanted injury from heating effects).

Transarterial chemoembolization (TACE) relies on selective embolization of a segmental or lobar hepatic artery with chemotherapeutic drug-eluting microspheres to treat HCC. TACE is recommended by multiple major liver societies as the first-line therapy for large or multifocal HCC, or in candidates with extrahepatic spread who are not suitable for surgical management (Fig. 8). TACE has been shown to increase life expectancy and overall quality of life in patients with advanced HCC (44). In comparison with traditional chemoembolization, drug-eluting microspheres have the advantage of sustained release of the chemotherapeutic agent over a long period of time. Selective or superselective catheterization of the hepatic arterial branches supplying HCC is performed to maximize delivery of drug-eluting microspheres in the tumor, and thereby minimizing the exposure of normal hepatic parenchyma. The administration of radioactive Y-90 beta-emitting microspheres is another technique for arterial-directed tumor therapy, depositing a lethal radiation dose locally to the tumor. This technique requires highly regional selective embolization of the HCC to minimize morbidity from unwanted radioactive dosing of the adjacent functional liver. In addition, prophylactic bland embolization of the gastroduodenal artery and other extrahepatic vessels is essential prior to Y-90 microspheres administration to prevent reflux of the radioactive microspheres into the gastric vascular supply, which may cause intractable radiation ulcers (45).

Treatment response of HCC following transarterial chemo- or radioembolization has been assessed through reduction of tumor volume; however, reliance on changes in tumor size is a relatively slow and incomplete indicator of tumor response. Postradioembolization effects, in particular, may cause enlargement of the treated region of the tumor due to radiation induced necrosis, with the potential for an erroneous interpretation of disease progression when relying on size alone. In contrast to measuring changes in tumor size, assessment of tumor vascularity using contrast-enhanced MRI has been shown to provide an earlier and more accurate biomarker of tumor response. Prior studies have demonstrated that any residual vascularized soft tissue nodules within the treated tumor volume are indicative

Table 3. Liver Imaging-Reporting and Data System (LI-RADS)

Category	Concept	Imaging findings
LR 1	Definitely benign	• Imaging features diagnostic of a benign entity or • Definite disappearance at follow-up in the absence of treatment
LR 2	Probably benign	• Imaging features suggestive but NOT diagnostic of a benign entity
LR 3	Intermediate probability for HCC Both HCC and benign entity have moderate probability	• Not definite mass Includes nodule-like hepatic arterial phase hyperenhancement • Definite mass 1. Mass with hepatic arterial phase hypo- or isoenhancement a) <20 mm mass with ≤1 of following: washout, capsule, threshold growth b) ≥20 mm mass with none of following: washout, capsule, threshold growth 2. Mass with hepatic arterial phase hyperenhancement a) <20 mm mass with none of following: washout, capsule, threshold growth
LR 4	Probably HCC High but not 100% probability of HCC	• LR 4A (<20 mm mass) 1. Mass with arterial phase hypo- or iso-enhancement and ≥2 of following: "wash out", "capsule", threshold growth 2. Mass with arterial phase hyperenhancement a) <10 mm mass with ≥1 of following: washout, capsule, threshold growth or b) 10–19 mm mass with only 1 of following: washout, capsule, threshold growth LR 4B (≥20 mm mass) • LR 4B (≥20 mm mass) 1. Mass with arterial phase hypo- or isoenhancement with ≥1 of following: wash out, capsule, threshold growth 2. Mass with arterial phase hyperenhancement and none of following: washout, capsule, threshold growth
LR 5	Definitely HCC	• LR 5A (10–19 mm mass) a) Mass with arterial phase hyperenhancement 10–19 mm mass with ≥2 of following: washout, capsule, threshold growth LR 5B (≥20 mm mass) b) Mass with arterial phase hyperenhancement ≥ 20 mm mass with ≥ 1 of following: washout, capsule, threshold growth • LR 5V Definitely HCC with tumor in vein

HCC, hepatocellular carcinoma.

of residual viable disease (46). Earlier studies have also demonstrated that treated tumors normally will develop an enhancing halo of liver tissue adjacent to the outer margins of the tumor. It has been shown that this enhancing halo may persist around the embolized treatment cavity for several months, and this finding should not be mistaken for tumor recurrence (46–48).

Directly administered percutaneous ablative therapy is effective for small (<4 cm) HCC. There are various forms of direct ablation that includes intralesional injection of toxic agents (chemicals, radioactive isotopes, or chemotherapeutic drugs), application of an energy source capable of producing heat (such as radiofrequency and microwave), and also the use of tumor cooling and freezing (cryotherapy). All of these techniques induce eventual tissue necrosis.

Following direct ablative techniques, the necrotic tumor cavity becomes hyperintense relative to the pretherapy tumor signal and to the surrounding parenchyma on T1-weighted images. As with the arterial embolization methods, adequate treatment response is determined by the absence of any residual arterial enhancement within the tumor. A recurrent tumor may appear as nodular arterial enhancing foci adjacent to the edges of the devascularized treatment focus, typically showing delayed phase washout and pseudocapsule enhancement, as is characteristic for focal HCC (49–51).

Regardless of the therapeutic approach for HCC, repeated longitudinal imaging is required to adequate-

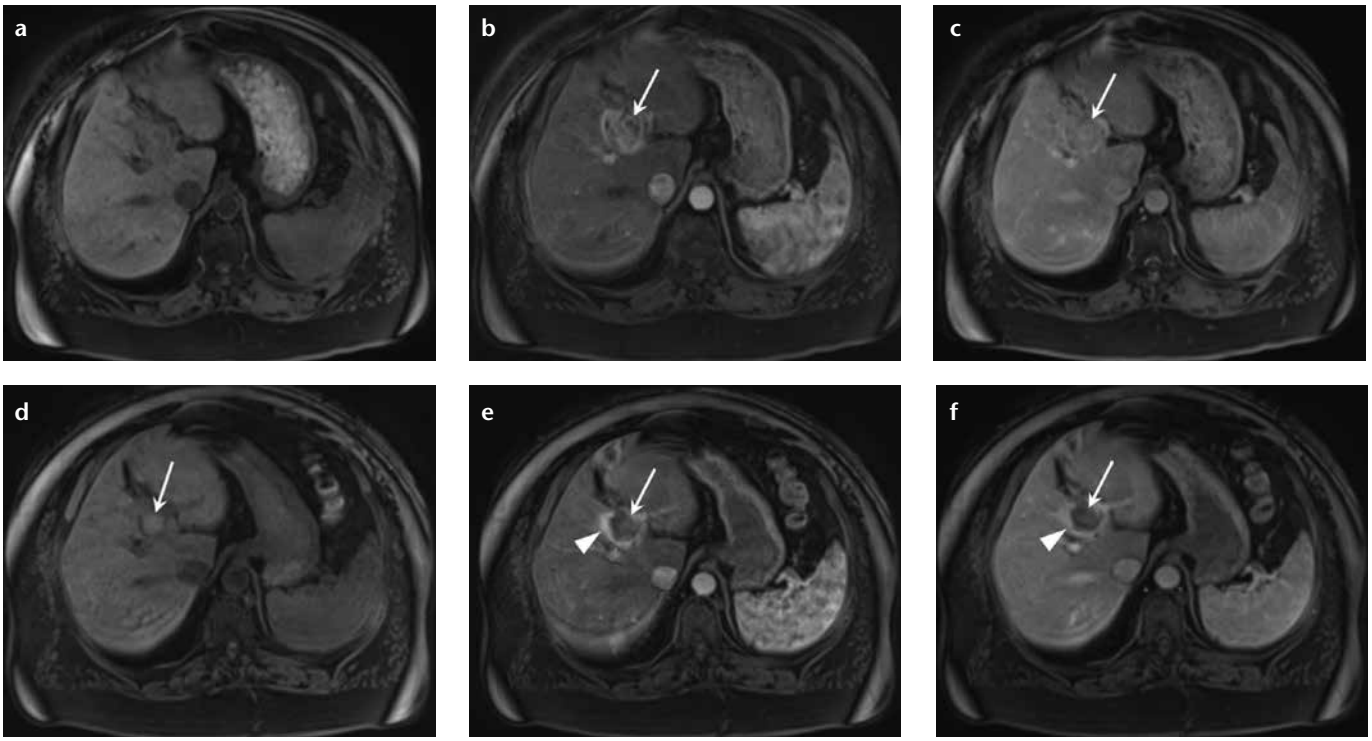

Figure 8. a–f. MR images in a 59-year-old male with cirrhosis secondary to nonalcoholic steatohepatitis show an HCC in segment VII of the liver. Precontrast **(a)** and arterial phase **(b)** T1-weighted 3D GRE images show enhancement on the arterial phase (**b,** *arrow*) with washout on the delayed phase T1-weighted 3D GRE image (**c,** *arrow*). The patient was reimaged three months after chemoembolization to assess response to treatment; precontrast **(d)**, arterial phase **(e)**, and delayed phase **(f)** images show no abnormal arterial enhancing tissue within the treatment site to suggest residual disease (**e, f,** *arrows*). Note the tumor demonstrated elevated signal on precontrast images, suggesting coagulative necrosis following treatment (**d,** *arrow*). There is also reactive, perilesional enhancement on arterial and delayed phase images consistent with treatment related effects (**e, f,** *arrowheads*).

ly monitor treatment response, plan consecutive therapy, and to evaluate for potential complications. The European Association for the Study of the Liver now endorses imaging features, including loss of arterial enhancement by tumor, as a marker for response to treatment. AASLD and the Journal of the National Cancer Institute (AASLD-JNCI) have modified the Response Evaluation Criteria in Solid Tumors (mRECIST) to incorporate enhancement features on MRI as an indicator of treatment response, in combination with size measurements (3, 7, 52).

Conclusion

In summary, the collective body of literature supports that HCC is a disease mostly observed in CLD and is best treated using liver transplantation within the Milan Criteria. To ensure patients are detected with treatable disease, surveillance screening is advocated using imaging in place of biopsy. GBCA-enhanced multiphase MRI (with an accurately timed arterial phase) is an extremely sensitive and specific imaging technique for HCC screening. Arterial enhancement of tumor is also a marker for viability and can be used to track tumor response to localized chemo-ablative therapies. Future directions include newer MRI techniques that may serve as biomarkers for tumor behavior that may be used to either extend transplant therapy to patients who would otherwise be beyond the Milan criteria or to exclude patients who would be likely to have disease recurrence even within the Milan criteria. Other future directions include automated MRI systems that will improve reproducible optimized technique across different imaging centers. The latest developments in 3D GRE are designed to facilitate rapid perfusion imaging of liver tumors with improved image quality and achievable even while a patient is breathing freely, with the expectation that this would achieve even higher levels of sensitivity and specificity for HCC in even the most challenging patients.

Conflict of interest disclosure

The authors declared no conflicts of interest.

References

1. Altekruse SF, McGlynn KA, Reichman ME. Hepatocellular carcinoma incidence, mortality, and survival trends in the United States from 1975 to 2005. J Clin Oncol 2009; 27:1485–1491. [CrossRef]
2. Ayyappan AP, Jhaveri KS. CT and MRI of hepatocellular carcinoma: an update. Expert Rev Anticancer Ther 2010; 10:507–519. [CrossRef]
3. Willatt JM, Hussain HK, Adusumilli S, Marrero JA. MR Imaging of hepatocellular carcinoma in the cirrhotic liver: challenges and controversies. Radiology 2008; 247:311–330. [CrossRef]
4. Mazzaferro V, Regalia E, Doci R, et al. Liver transplantation for the treatment of small hepatocellular carcinomas in patients with cirrhosis. N Engl J Med 1996; 334:693–699. [CrossRef]
5. Digumarthy SR, Sahani DV, Saini S. MRI in detection of hepatocellular carcinoma (HCC). Cancer Imaging 2005; 5:20–24. [CrossRef]
6. Yu NC, Chaudhari V, Raman SS, et al. CT and MRI improve detection of hepatocellular carcinoma, compared with ultrasound alone, in patients with cirrhosis. Clin Gastroenterol Hepatol 2011; 9:161–167. [CrossRef]

7. Ayuso C, Rimola J, Garcia-Criado A. Imaging of HCC. Abdom Imaging 2012; 37:215–230. [CrossRef]
8. Kim KA, Kim MJ, Choi JY, Chung YE. Development of hepatocellular carcinomas in patients with absence of tumors on a prior ultrasound examination. Eur J Radiol 2012; 81:1450–1454. [CrossRef]
9. Lee KH, O'Malley ME, Haider MA, Hanbidge A. Triple-phase MDCT of hepatocellular carcinoma. AJR Am J Roentgenol 2004; 182:643–649. [CrossRef]
10. Solomon R. Contrast-induced acute kidney injury: is there a risk after intravenous contrast? Clin J Am Soc Nephrol 2008; 3:1242–1243. [CrossRef]
11. Pitton MB, Kloeckner R, Herber S, Otto G, Kreitner KF, Dueber C. MRI versus 64-row MDCT for diagnosis of hepatocellular carcinoma. World J Gastroenterol 2009; 15:6044–6051. [CrossRef]
12. Purysko AS, Remer EM, Coppa CP, Leão Filho HM, Thupili CR, Veniero JC. LI-RADS: a case-based review of the new categorization of liver findings in patients with end-stage liver disease. Radiographics 2012; 32:1977–1995. [CrossRef]
13. Burrel M, Llovet JM, Ayuso C, et al. MRI angiography is superior to helical CT for detection of HCC prior to liver transplantation: an explant correlation. Hepatology 2003; 38:1034–1042. [CrossRef]
14. Khalili K, Kim TK, Jang HJ, et al. Optimization of imaging diagnosis of 1-2 cm hepatocellular carcinoma: an analysis of diagnostic performance and resource utilization. J Hepatol 2011; 54:723–728. [CrossRef]
15. Becker-Weidman DJ, Kalb B, Sharma P, et al. Hepatocellular carcinoma lesion characterization: single-institution clinical performance review of multiphase gadolinium-enhanced MR imaging--comparison to prior same-center results after MR systems improvements. Radiology 2011; 261:824–833. [CrossRef]
16. Martin DR, Krishnamoorthy S, Kalb B, et al. Decreased incidence of NSF in patients on dialysis after changing gadolinium contrast-enhanced MRI protocols. J Magn Reson Imaging 2010; 31:440–446. [CrossRef]
17. Catalano OA, Choy G, Zhu A, Hahn PF, Sahani DV. Differentiation of malignant thrombus from bland thrombus of the portal vein in patients with hepatocellular carcinoma: application of diffusion-weighted MR imaging. Radiology 2010; 254:154–162. [CrossRef]
18. Earls JP, Rofsky NM, DeCorato DR, Krinsky GA, Weinreb JC. Hepatic arterial-phase dynamic gadolinium-enhanced MR imaging: optimization with a test examination and a power injector. Radiology 1997; 202:268–273.
19. Sharma P, Kitajima HD, Kalb B, Martin DR. Gadolinium-enhanced imaging of liver tumors and manifestations of hepatitis: pharmacodynamic and technical considerations. Top Magn Reson Imaging 2009; 20:71–78. [CrossRef]
20. OPTN policy management. Available at: http://optn.transplant.hrsa.gov/policiesAndBylaws/poli cies.asp. Accessed March 1, 2012.
21. Lauenstein TC, Sharma P, Hughes T, Heberlein K, Tudorascu D, Martin DR. Evaluation of optimized inversion-recovery fat-suppression techniques for T2-weighted abdominal MR imaging. J Magn Reson Imaging 2008; 27:1448–1454. [CrossRef]
22. Udayasankar UK, Martin D, Lauenstein T, et al. Role of spectral presaturation attenuated inversion-recovery fat-suppressed T2-weighted MR imaging in active inflammatory bowel disease. J Magn Reson Imaging 2008; 28:1133–1140. [CrossRef]
23. Seale MK, Catalano OA, Saini S, Hahn PF, Sahani DV. Hepatobiliary-specific MR contrast agents: role in imaging the liver and biliary tree. Radiographics 2009; 29:1725–1748. [CrossRef]
24. Le Moigne F, Durieux M, Bancel B, et al. Impact of diffusion-weighted MR imaging on the characterization of small hepatocellular carcinoma in the cirrhotic liver. Magn Reson Imaging 2012; 30:656–665. [CrossRef]
25. Qu JR, Li HL, Shao NN, et al. Additional diffusion-weighted imaging in the detection of new, very small hepatocellular carcinoma lesions after interventional therapy compared with conventional 3 T MRI alone. Clin Radiol 2012; 67:669–674. [CrossRef]
26. Saranathan M, Rettmann DW, Hargreaves BA, Clarke SE, Vasanawala SS. Differential Subsampling with Cartesian Ordering (DISCO): a high spatio-temporal resolution Dixon imaging sequence for multiphasic contrast enhanced abdominal imaging. J Magn Reson Imaging 2012; 35:1484–1492. [CrossRef]
27. Mori K, Yoshioka H, Takahashi N, et al. Triple arterial phase dynamic MRI with sensitivity encoding for hypervascular hepatocellular carcinoma: comparison of the diagnostic accuracy among the early, middle, late, and whole triple arterial phase imaging. AJR Am J Roentgenol 2005; 184:63–69. [CrossRef]
28. Chandarana H, Block T, Rosenkrantz A, et al. Free-breathing radial 3D fat-suppressed T1-weighted gradient echo sequence: a viable alternative for contrast-enhanced liver imaging in patients unable to suspend respiration. Invest Radiol 2011; 46:648–653. [CrossRef]
29. Berman BP, Li Z, Altbach MI, et al. How to stack stars: a variable center-dense k-space trajectory for 3D MRI. Paper presented at: 2013 Annual Meeting of International Society for Magnetic Resonance in Medicine; April 23, 2013; Salt Lake City, USA.
30. Lauenstein TC, Salman K, Morreira R, et al. Gadolinium-enhanced MRI for tumor surveillance before liver transplantation: center-based experience. AJR Am J Roentgenol 2007; 189:663–670. [CrossRef]
31. Kelekis NL, Semelka RC, Worawattanakul S, et al. Hepatocellular carcinoma in North America: a multiinstitutional study of appearance on T1-weighted, T2-weighted, and serial gadolinium-enhanced gradient-echo images. AJR Am J Roentgenol 1998; 170:1005–1013. [CrossRef]
32. Hussain HK, Londy FJ, Francis IR, et al. Hepatic arterial phase MR imaging with automated bolus-detection three-dimensional fast gradient-recalled-echo sequence: comparison with test-bolus method. Radiology 2003; 226:558–566. [CrossRef]
33. Van den Bos IC, Hussain SM, Dwarkasing RS, et al. MR imaging of hepatocellular carcinoma: relationship between lesion size and imaging findings, including signal intensity and dynamic enhancement patterns. J Magn Reson Imaging 2007; 26:1548–1555. [CrossRef]
34. Kalb B, Becker-Weidman DJ, Chundru S, et al. Magnetic resonance imaging of HCC: predictive findings of post-transplant tumor recurrence in a screening population. Paper presented at: 2012 Annual Meeting of International Society for Magnetic Resonance in Medicine; May 8, 2012; Melbourne, Australia.
35. Nakanishi M, Chuma M, Hige S, et al. Relationship between diffusion-weighted magnetic resonance imaging and histological tumor grading of hepatocellular carcinoma. Ann Surg Oncol 2012; 19:1302–1309. [CrossRef]
36. Kanematsu M, Semelka RC, Leonardou P, Mastropasqua M, Lee JK. Hepatocellular carcinoma of diffuse type: MR imaging findings and clinical manifestations. J Magn Reson Imaging 2003; 18:189–195. [CrossRef]
37. Myung SJ, Yoon JH, Kim KM, et al. Diffuse infiltrative hepatocellular carcinomas in a hepatitis B-endemic area: diagnostic and therapeutic impediments. Hepatogastroenterology 2006; 53:266–270.
38. American College of Radiology. Quality and safety resources: Liver Imaging–Reporting and Data System. Available at: http://www.acr.org/Quality- Safety/Resources/LIRADS. Accessed March 1, 2011.
39. Cruite I, Tang A, Sirlin CB. Imaging-based diagnostic systems for hepatocellular carcinoma. AJR Am J Roentgenol 2013; 201:41–55. [CrossRef]
40. Yao FY, Xiao L, Bass NM, Kerlan R, Ascher NL, Roberts JP. Liver transplantation for hepatocellular carcinoma: validation of the UCSF-expanded criteria based on preoperative imaging. Am J Transplant 2007; 7:2587–2596. [CrossRef]
41. Stigliano R, Burroughs AK. Should we biopsy each liver mass suspicious for HCC before liver transplantation?--no, please don't. J Hepatol 2005; 43:563–568. [CrossRef]

42. Chang S, Kim SH, Lim HK, et al. Needle tract implantation after percutaneous interventional procedures in hepatocellular carcinomas: lessons learned from a 10-year experience. Korean J Radiol 2008; 9:268–274. [CrossRef]
43. Chundru S, Kalb B, Arif-Tiwari H, Sharma P, Costello J, Martin DR. MRI of diffuse liver disease: the common and uncommon etiologies. Diagn Interv Radiol 2013; 19:479–487.
44. Van Ha TG. Transarterial chemoembolization for hepatocellular carcinoma. Semin Intervent Radiol 2009; 26:270–275. [CrossRef]
45. Kalva SP, Thabet A, Wicky S. Recent advances in transarterial therapy of primary and secondary liver malignancies. Radiographics 2008; 28:101–117. [CrossRef]
46. Kalb B, Chamsuddin A, Nazzal L, Sharma P, Martin DR. Chemoembolization follow-up of hepatocellular carcinoma with MR imaging: usefulness of evaluating enhancement features on one-month post-therapy MR imaging for predicting residual disease. J Vasc Interv Radiol 2010; 21:1396–1404. [CrossRef]
47. Khankan AA, Murakami T, Onishi H, et al. Hepatocellular carcinoma treated with radio frequency ablation: an early evaluation with magnetic resonance imaging. J Magn Reson Imaging 2008; 27:546–551. [CrossRef]
48. Lau WY, Yu SC, Lai EC, Leung TW. Transarterial chemoembolization for hepatocellular carcinoma. J Am Coll Surg 2006; 202:155–168. [CrossRef]
49. Kim SK, Lim HK, Kim YH, et al. Hepatocellular carcinoma treated with radio-frequency ablation: spectrum of imaging findings. Radiographics 2003; 23:107–121. [CrossRef]
50. Lau WY, Leung TWT, Yu SCH, Ho SKW. Percutaneous local ablative therapy for hepatocellular carcinoma. Ann Surg 2003; 273:171–179. [CrossRef]
51. Tatli S, Tapan U, Morrison PR, Silverman SG. Radiofrequency ablation: technique and clinical applications. Diagn Interv Radiol 2012; 18:508–516.
52. Lencioni R, Llovet JM. Modified RECIST (mRECIST) assessment for hepatocellular carcinoma. Semin Liver Dis 2010; 30:52–60. [CrossRef]